# Enhancement of $^5D_0$-$^7F_J$ Emissions of $Eu^{3+}$ Ions in the Vicinity of Polymer-Protected Au Nanoparticles in Sol−Gel-Derived $B_2O_3$−$SiO_2$ Glass

**Tomokatsu Hayakawa,* Kazunori Furuhashi, and Masayuki Nogami**

*Ceramic Division, Department of Materials Science and Engineering, Nagoya Institute of Technology, Gokiso, Showa, Nagoya 466-8555, Japan*

*Received: April 22, 2004*

The paper reports the enhanced photoluminescence of trivalent europium ($Eu^{3+}$) ions in the vicinity of nanometer-sized metal particles in glasses. In this study, gold (Au) colloids synthesized in solution were introduced into a borosilicate ($B_2O_3$−$SiO_2$) glass matrix together with $Eu^{3+}$ ions via a sol−gel route. To control in size and protect Au colloids two types of polymers—poly(vinylpyrrolidone) (PVP) and polyacryronitorile (PAN)—were used. As a result, PVP provided excellent homogeneity of Au nanoparticles in the hybrid gel. A novel finding on its photoluminescence properties is that a heat treatment of the gel at 400 °C led to a great enhancement of $Eu^{3+}$ fluorescence under a long ultraviolet excitation, six times higher than without Au nanoparticles, accompanied with a broad fluorescence around 400 nm due to carbonyl moieties of PVP. On the contrary, when the carbonyl groups were removed by heat treatment at temperatures higher than 400 °C, a conspicuous decrease in the relative intensity of $Eu^{3+}$ fluorescence was observed, regardless of the presence of Au nanoparticles. Since a group of carbonyl terminations, when coordinated to $Eu^{3+}$ ions (>C═O → $Eu^{3+}$), can be an energy donor, these observations showed that $Eu^{3+}$ ions were strongly excited by the energy transfer from C═O groups, which were placed in enhanced local fields near Au nanoparticles due to higher orders of surface plasmon resonances.

## 1. Introduction

Surface plasmon resonance (SPR) of metal nanoparticles, which is of importance as one of the elemental excitations in solid-state quantum physics,[1,2] provides not only a great enhancement of optical third-order nonlinear susceptibility of metal ("*inside-field effect*")[3−5] but also an increase in the local electromagnetic field strength around a nanometer-sized metal ("*outside-field effect*").[6−8] So far we are focused on the latter effect, and the enhancement of trivalent europium ($Eu^{3+}$) fluorescence was previously reported.[9−11] In several of our research studies , silver ($Ag^+$) and $Eu^{3+}$ ions were co-doped in silica glass by a sol−gel method and the following heat-treatment in a reduction atmosphere gave rise to the precipitation of Ag nanoparticles.

In this work a nanometer size of gold (Au) colloids in solution were incorporated into a borosilicate amorphous network of $10B_2O_3$−$90SiO_2$ together with $Eu^{3+}$ ions via a sol−gel route. To control Au nanoparticles in size and obtain their good stability through the whole of synthesis, two different types of polymers (poly(vinylpyrrolidone) (PVP) and polyacrylonitrile (PAN))[12,13] were utilized. The sizes of the particles in a starting solution and gel−glasses were monitored by optical extinction spectra and analyzed by Mie-Drude theory.[14−16] One of the aims of this work is to investigate the effects of Au nanoparticles on $Eu^{3+}$ fluorescence under photoexcitation of a long ultraviolet (UV) light, which is higher in energy than the first order (dipole) of SPR of Au nanoparticles. Influences of carbon-related phosphors originating from protective polymers of Au nanoparticles are also studied at various temperatures in heat-treatment for the fabricated gels of $10B_2O_3$−$90SiO_2$ doped with $Eu^{3+}$ ions and polymer-protected Au nanoparticles. It will be shown that $Eu^{3+}$ fluorescence of $^5D_0$-$^7F_J$ transitions is enhanced in the presence of such Au nanoparticles and we shall discuss the enhanced $Eu^{3+}$ fluorescence in terms of energy transfer from a carbonyl chromophore (>C═O) to $Eu^{3+}$ ions in a local field enhancement near nanometer-sized Au particles due to higher orders of SPR excitations.

## 2. Experiment

Figure 1 shows a flowchart of the sol−gel synthesis for $10B_2O_3$−$90SiO_2$ gels containing both polymer-protected Au nanoparticles and $Eu^{3+}$ ions. As a protective organic agent of Au nanoparticles, we selected two different types of organic polymers—PVP (K-90, $M_W \sim 360\,000$; Kishida Chem. Co.) and PAN ($M_W \sim 86\,200$; Aldrich), for which it is known to have affinitive moieties of a lone electron pair of tri-coordinated nitrogen and cyano-group −CN to Au ions, respectively. The starting materials for the synthesis of nanometer-sized Au colloids in solution were $HAuCl_4$ (Kishida Chem. Co.), PVP (or PAN), and $KBH_4$ (Kishida Chem. Co.). For PVP-protected Au sol, 2.5 mL of 2.0 mM $HAuCl_4$ solution was added to a mixture of ethanol and distilled water with PVP (ethanol: 15 mL, water: 30 mL, PVP: 22.4 mg). For the reduction of $AuCl_4^-$, 2.5 mL of 20 mM $KBH_4$ solution was injected into the solution so that the color of the Au sol was turned from yellow to light red (A-PVP; see Figure 2a). ([vp]/[Au] = 40, where [vp] = a molar amount of vinylpyrrolidone groups.) For PAN-protected Au sol, 11.2 mg of PAN was added to 45 mL of *N*,*N*-dimethylformamide (DMF; Nacalai Tesque, Inc.), which was mixed with 2.5 mL of 2.0 mM $HAuCl_4$ solution. Addition of 2.5 mL of 20 mM $KBH_4$ solution allowed PAN-protected Au sol to be formed (A-PAN; see Figure 2b). ([an]/[Au] = 40, where [an] = a molar amount of $-CH_2-CH(CN)-$.) [vp]/[Au]

* Corresponding author. E-mail: hayatomo@nitech.ac.jp.

10.1021/jp048247w CCC: $27.50 
Published on Web 07/13/2004

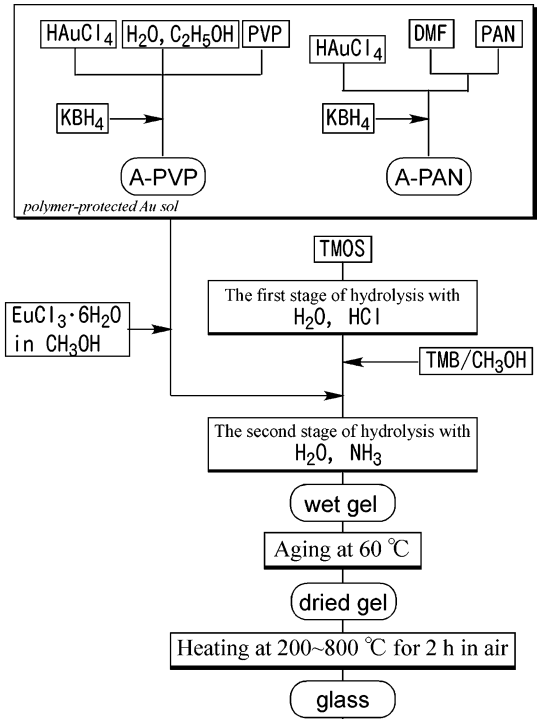


**Figure 1.** Flowchart of the sample preparation of sol−gel derived $10B_2O_3-90SiO_2$ containing $Eu^{3+}$ and polymer (PVP, PAN)-protected Au nanoparticles.

and [an]/[Au] had a great influence on the particle size of Au, and the ratio is fixed at 40 in this study.

The glass of $10B_2O_3-90SiO_2$ was selected as a matrix for the incorporation of Au nanoparticles because of its high densification and low sintering temperature.[17] The chemicals for the glass matrix synthesis were tetramethylortholsilicate, $Si(OCH_3)_4$ (TMOS; Colcoat Co.) and trimethylborate, $C_3H_9BO_3$ (TMB; Fuluka). At first, TMOS was added dropwise to distilled water that included a small amount of HCl ($TMOS:H_2O:HCl = 1:4:1 \times 10^{-3}$ M), and stirred for 1 h. TMB in methanol ($C_3H_9BO_3/CH_3OH = 2.5$ in volume) was added dropwise with further stirring for 1 h (B). The molar ratio for fabricating the $10B_2O_3-90SiO_2$ glass composition is $TMOS:TMB:CH_3OH = 9:2:2.23$. The polymer-protected Au sol (A-PVP or A-PAN) was mixed with a 5 g of methanol dissolving $EuCl_3 \cdot 6H_2O$ (Kishida Chem. Co.), and added to the $B_2O_3-SiO_2$ sol (B). The concentration of $Eu_2O_3$ was set to 2 wt %. The color of the solution remained light red, showing good stability of Au nanoparticles. And then, distilled water including $NH_3$ ($TMOS:H_2O:NH_3 = 1:7:5 \times 10^{-2}$ M) was added with stirring for 15 min. It took 3 days to obtain a stiff gel. Then, the gel was transferred into an oven at 60 °C and kept for various lengths of time. Finally, the gel was heated in air at the rate of 50 °C/h and kept for 2 h in the temperature range 200−800 °C, labeled by AuEu−BS (Au concentration was $4 \times 10^{-3}$ wt %). The gel-to-glass transformation was monitored in a Raman scattering investigation by using a micro Raman spectrometer (JASCO, NRS-2000). For comparison, samples not incorporated with gold nanoparticles but with the protective polymer and $Eu^{3+}$ ions were prepared, which were denoted by Eu−BS.

Optical absorption measurements were employed in the range between 200 and 800 nm at room temperature with a UV−Vis spectrophotometer (JASCO, V-570). Transmission electron microscopy (TEM) images were also collected with an electron microscope (JEOL, JEM-2000EX) operated at an accelerated voltage of 200 kV. Photoluminescence (PL) measurements were carried out with use of a nitrogen gas ($N_2$) laser as an excitation source (Nippon Laser Co., LN203C; $\lambda = 337.1$ nm, pulse width < 1 ns). The detection system was constructed of a high-resolution monochromator (Jobin-Yvon, HR-320) and image-intensified charge couple device (ICCD) camera system (ORIEL instrument, InstaSpect V). The excitation spectra of $Eu^{3+}$ emission were measured at room temperature with a 500 W Xe-lamp (Ushio, UXL-500D) and monochromator (Jobin-Yvon, H-20) controlled by a computer.

## 3. Results

**3.1. Introduction of Polymer-Protected Au Colloids into the $B_2O_3-SiO_2$ Glass Matrix.** Figure 2, parts c and d, displays photographs of the fabricated borosilicate glasses incorporated with (a) PVP- and (b) PAN-protected Au sol, respectively. When starting with PVP-protection of Au nanoparticles in sol we can obtain a homogeneous and red-colored monolith, while the choice of PAN leads to phase separation of the polymer-protected Au nanoparticles. The molecular structures of PVP and PAN are given in Figure 2, parts e and f, respectively. Previous research[18,19] verifies that the combination of PVP ($-(CH_2CH(NC_3H_3CO)_n-$) and silicate network provides homogeneous inorganic/organic monoliths or hybrid gels, because conjugated $\pi$ electrons in the carbonyl bond have a tendency to hydrogen-bond with hydroxyl (OH) groups coming from the $SiO_2$ matrix. On the other hand, PAN has better properties for Au nanoparticle protection than PVP, resulting in a narrower size-distribution of polymer-protected Au nanoparticles with smaller mean size (a few nanometers in diameter).[12] However, PAN ($-(CH_2CH(CN))_n-$) has no hydrophilic moieties so that the three-dimensional framework of silicate glass cannot be hybridized with PAN. Thus, in the latter part of our experiment PVP is thoroughly used.

In the preparation of $B_2O_3-SiO_2$ gel doped with polymer-protected Au nanoparticles, the aging time at 60 °C should not be much longer than 3 days. Otherwise, the Au nanoparticles disappear, and as a result the characteristic color of light red is lost. It is because the initial gel includes acidic molecules such as orthoborate and pyroborate coming from hydrolyzed trimethylborate (see Figure 3), which may destroy the synthesized Au nanoparticles. The gel formation is so fast that the aging time should be suppressed to be a few days. By the gentle warming in an oven the inorganic gel is promoted to be polymerized and the homogeneous hybrid can be obtained successfully.

**3.2. Mie-Drude Analysis of Au Nanoparticles.** Figure 4 shows absorption spectra of PVP-protected Au nanoparticles in sol and in $10B_2O_3-90SiO_2$ gels including only PVP-protected Au nanoparticles (Au−BS). A band around 520 nm is due to the light scattering extinction of SPR in Au nanoparticles. The clear peak without a tail to longer wavelength shows that the particles exist individually. According to the simple Mie-Drude theory in a classical approach, the extinction peak due to metal nanoparticles in the absorption spectra is expressed by[9,10,14−16,20]

$$\alpha(\omega) = \frac{9qn^3}{c(1+2n^2)} \frac{\omega^2\omega_r^2/\tau}{(\omega^2-\omega_r^2)^2 + (\omega_r^2/\omega\tau)^2}$$

where $q$ is the volume fraction of metal particles, and $\omega_r$ is the Mie's resonant frequency of surface plasmon ($c$ is the light velocity in a vacuum, and $n$ is the refractive index of surrounding). This only holds when the particle size is quite smaller than an incident wavelength. The full width at half-maximum

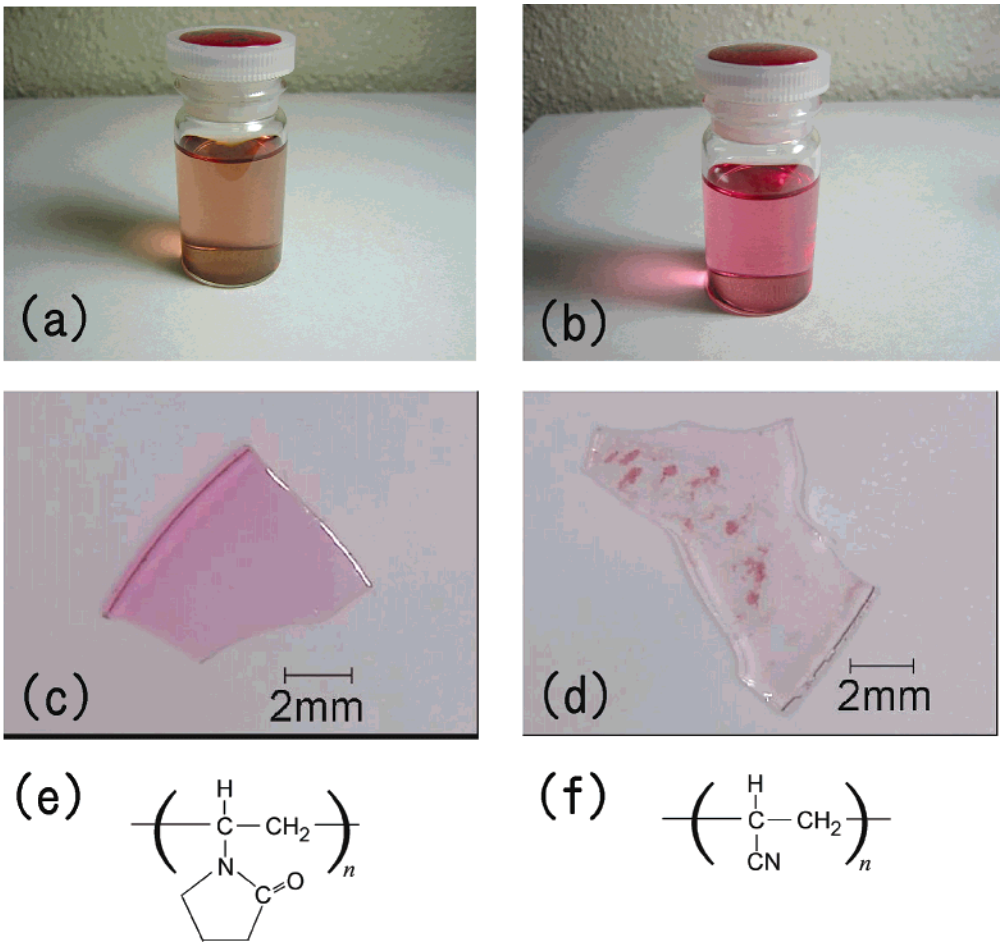


**Figure 2.** Photographs of (a) A-PVP sol, (b) A-PAN sol, and (c), (d) the fabricated borosilicate glasses incorporated with A-PVP and A-PAN, respectively, which were heated at 700 °C for 2 h in air; (e), (f) chemical structures of PVP and PAN, respectively.

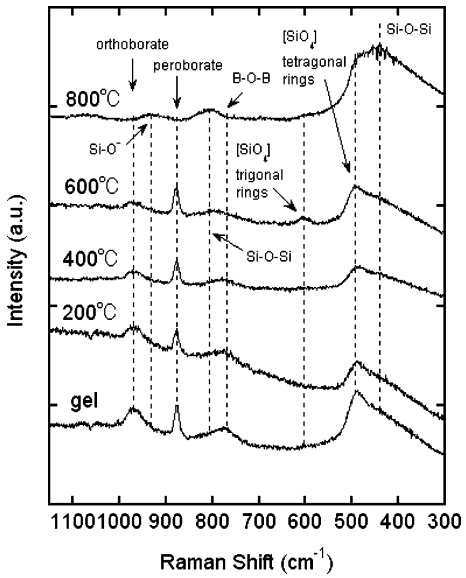


**Figure 3.** Raman spectra of sol−gel-derived $10B_2O_3-90SiO_2$, containing PVP-protected Au nanoparticles, heated at various temperatures for 2 h in air.

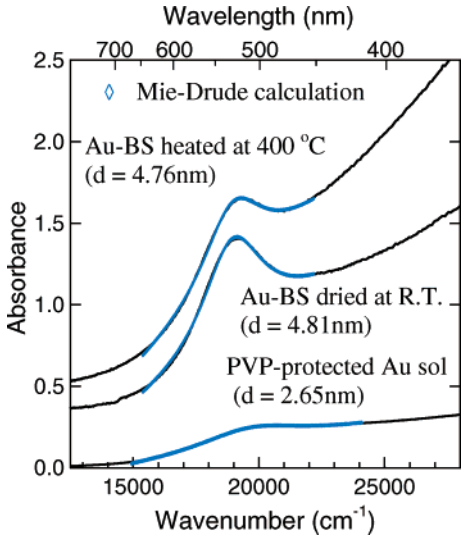


**Figure 4.** Optical absorption spectra of PVP-protected Au nanoparticles in sol and $10B_2O_3-90SiO_2$ gel-glass hybridized with PVP-protected Au nanoparticles (Au−BS).

(fwhm) $\Delta\omega$ for SPR is correlated with the relaxation time of conduction electrons $\tau$ through $\tau^{-1} \sim \Delta\omega$. As Doyle[16] and Kreibig et al.[21] proposed, for a spherical particle much smaller than the mean free path of the electrons in bulk material, $l_\infty$ (~42 nm at 273 K for bulk Au),[22] the collisions of the conduction electrons with the particle surfaces become important as an additional relaxation process, and the effective mean free path, $l$, is restricted by the representative length of the particle, $\sim R$. Thus, the relaxation time $\tau$ can be substituted for the collision time,

$$\tau_c = R/v_f \qquad (2)$$

where $v_f$ (= $1.39 \times 10^8$ cm/s) is the Fermi velocity for Au. Consequently, the particle size of metal nanoparticle can be

estimated from the fwhm of Mie's surface plasmon resonance in optical absorption spectra through

$$R = v_f/\Delta\omega \tag{3}$$

Additionally, the Mie resonant frequency is given by $\omega_r = \omega_p/(1 + 2n^2)^{1/2}$, in the first approximation of free electron behavior, where $\omega_p$ is a bulk plasmon frequency. However, bulk plasmon frequency for noble metals such as Ag, Au, and Cu does not coincide with free electron plasma frequency $(N_e/em_{opt})^{1/2}$ ($N_e$, $e$, and $m_{opt}$ represent the number, charge, and optical effective mass of conduction electrons, respectively), because of a tremendous contribution of the interband transition from the filled *d* band to the *sp* orbital. (The interband transition of Au is above 2.38 eV.[22,23]) The frequency of the surface plasmon resonance of a noble metal nanoparticle is determined from the original Mie equation, $(\epsilon_1 + \epsilon_M)^2 + \epsilon_2^2 =$ minimum.[14−16] It is noted that the contribution of interband transition to the peak position is given not only the imaginary part $\epsilon_2$ (energy dissipation) but also the real part $\epsilon_1$ (polarization) of metal. As a consequence, the surface plasmon of Au is located around 2.36 eV (∼525 nm), moreover slightly dependent on the refractive index of surrounding media through $\epsilon_M = n^2$. It can be seen that, in this case, the peak position of SPR is shifted from 526.8 nm in sol to 534.3 nm in gel and glass.

In Figure 4, the Mie-Drude fitting curves and estimated particle sizes $d = 2R$ from $R = v_f/\Delta\omega$ are also given. Initially, Au nanoparticles protected by PVP in solution have a small mean size of $d = 2.65$ nm; when incorporated with the $B_2O_3-SiO_2$ gel matrix, the particle grows to a size of $d = 4.81$ nm, possibly because of the coalescence of initial nanoparticles. The heat treatment at 400 °C in air leads to the stiffer glass network and combustion of PVP phase (an exothermic peak due to combustion of PVP was observed at 400 °C in DTA-TG measurement). The particle size is estimated to be 4.76 nm. These data show that the protection of Au nanoparticles by the polymer works well in the gel-to-glass transformation and each of the Au nanoparticles also remains to be isolated, even in the heat treatment at 400 °C, though the initial particle size in sol is not kept in the incorporation into the $B_2O_3-SiO_2$ gel matrix. Figure 5a displays a light-field image of TEM observation for the gel. The nanometer particles have a mean diameter of 6.4 nm and distribution to ±2.3 nm (see Figure 5b). The estimated particle size from optical absorption spectra is smaller than that obtained directly from TEM pictures. Such a discrepancy has been reported in several studies, which is thought to be due to chemical interface effect (CIE).[24]

**3.3. Enhanced $Eu^{3+}$ PL in the Vicinity of Au Nanoparticles under a Long UV Excitation.** Figure 6 shows PL spectra of AuEu−BS and Eu−BS heated at 200−800 °C in air under a long UV excitation of 337.1 nm (= 3.68 eV). In the region between 570 and 700 nm the PL bands due to $^5D_0$-$^7F_J$ ($J$ = 0, 1, 2, 3, ...) transitions of $Eu^{3+}$ ions can be observed (the assignment is given in the figure). It is found that AuEu−BS shows a stronger $Eu^{3+}$ fluorescence than Eu−BS except that heated at 600 °C in air. It should also be stressed that both AuEu−BS and Eu−BS contain the polymer of PVP and exhibit an additional broad luminescence around 400 nm. The peak position of the 400 nm-band is dependent on the heat treatment temperature, and when baked at temperatures higher than 800 °C the luminescence disappears (see Figure 7). The lifetime of the broad band is very fast and is found to be ∼25 ns. The carbonyl group (>C═O) of PVP, which is one of the most luminescent organic parts due to the conjugation of $\pi$ electrons, causes the observed broad luminescence.[25]

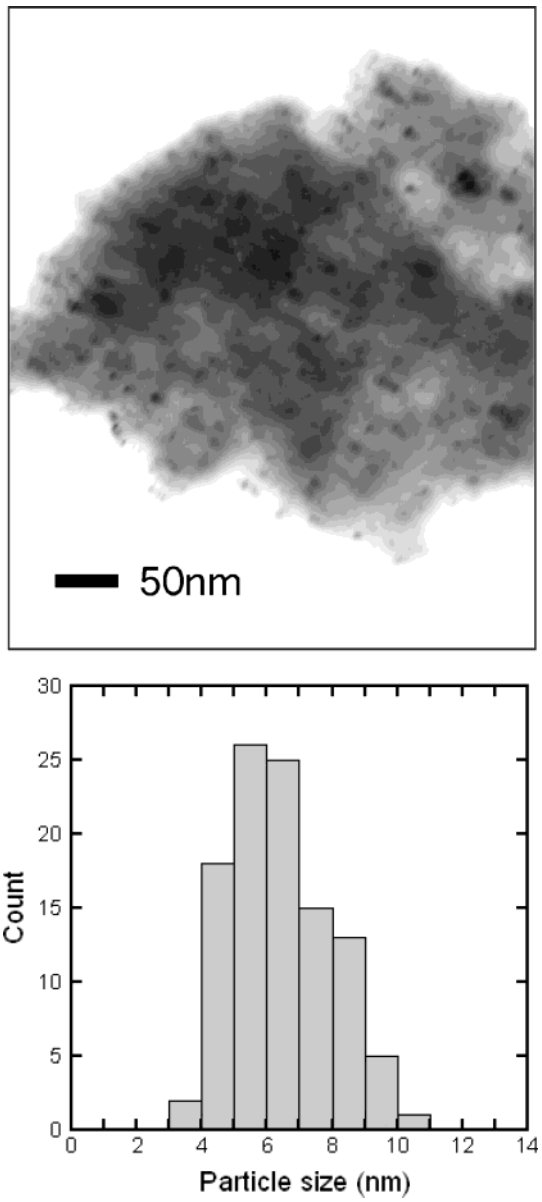


**Figure 5.** (a) Light-field image in TEM observation for the borosilicate gel containing PVP-protected Au nanoparticles (Au−BS), and (b) size-distribution of Au nanoparticles.

The excitation spectra monitored at 614 nm ($^5D_0$-$^7F_2$) for AuEu−BS heated at 400 and 800 °C are also measured, which are shown in Figure 8, parts a and b, respectively. Spectrum (a) in Figure 8 exhibits a broad excitation band due to the excitation of carbonyl chromphores, but spectrum (b) does not. The broad band includes a direct process of excitation−emission of carbonyl chromophores. As for AuEu−BS heated at 800 °C, $f-f$ transitions from $^7F_0$ to $^5D_{1-4}$, $^5L_6$, $^5G_{2,4}$, and $^5H_4$ levels of $Eu^{3+}$ ions are clearly observed. In absorption spectra (not shown here), there is not observed a substantial difference between AuEu−BS and Eu−BS except the resonance peak due to the surface plasmon, if they are heated at the same temperature.

To evaluate the enhancement of $^5D_0$-$^7F_J$ luminescence of $Eu^{3+}$ ions, we define an enhancement factor $f_E$ as

$$f_E = \frac{\sum_J I_J^{\text{AuEu-BS}}}{\sum_J I_J^{\text{Eu-BS}}} \tag{4}$$

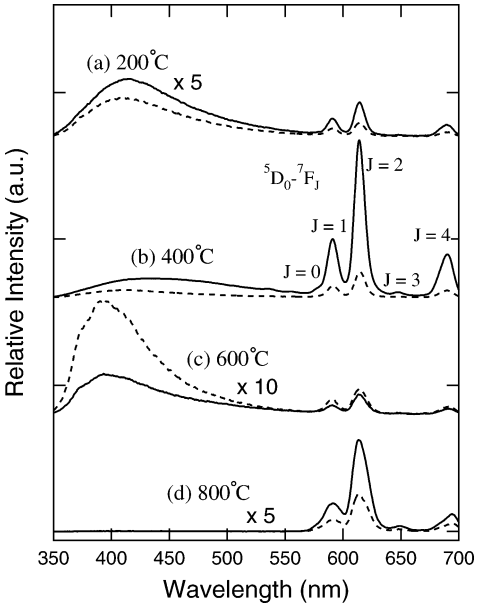


**Figure 6.** PL spectra of AuEu−BS (solid line) and Eu−BS (dashed line) samples heated at various temperatures for 2 h in air, which were recorded with a longer ICCD gate time of 5 ms.

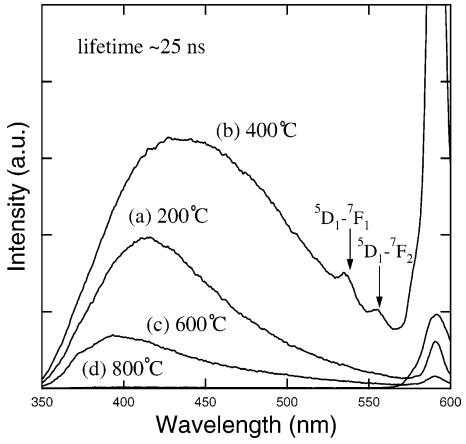


**Figure 7.** PL spectra of the broad band around 400 nm for AuEu−BS samples heated at various temperatures, which were recorded with a shorter ICCD gate time of 1 $\mu$s.

where $I_J$ denotes the integrated intensity of the $^5D_0$-$^7F_J$ band and the superscripts the sample names. Table 1 compiles $f_E$ and the total emission intensities, $R_{AuEu-BS} = \Sigma_J I_J^{AuEu-BS}$ and $R_{Eu-BS} = \Sigma_J I_J^{Eu-BS}$, for AuEu−BS and Eu−BS, respectively, in comparison with data when heated at 200 °C for Eu−BS. When baked at 400 °C the highest enhancement of ~6 is observed. However, the samples of AuEu−BS and Eu−BS heated at 600 °C show smaller $f_E$ of 0.76, and the relative intensities of $R_{AuEu-BS}$ and $R_{Eu-BS}$ are decreased. According to Levy et al. (see Table 1 in ref 26), when the $SiO_2$ gel doped with $Eu^{3+}$ ions was heated at elevated temperatures, the total emission intensities of $^5D_0$-$^7F_J$ transitions of $Eu^{3+}$ ions was increased because of the removal of hydroxyl and organic groups from the gel. On the contrary, since in our study the PVP is incorporated for both AuEu−BS and Eu−BS, the relative PL intensity of $^5D_0$-$^7F_J$ is drastically decreased at 600 °C, as shown in Table 1. This can be explained in the way that organics coming from PVP are at most decomposed at 600 °C but still remain on pore walls of AuEu−BS and Eu−BS gels, which therefore de-excite $Eu^{3+}$ ions in $^5D_0$ levels as killer sites, resulting in reducing PL intensity at 600 °C. However, if the gels are heated at temperatures higher than 600 °C, the residual

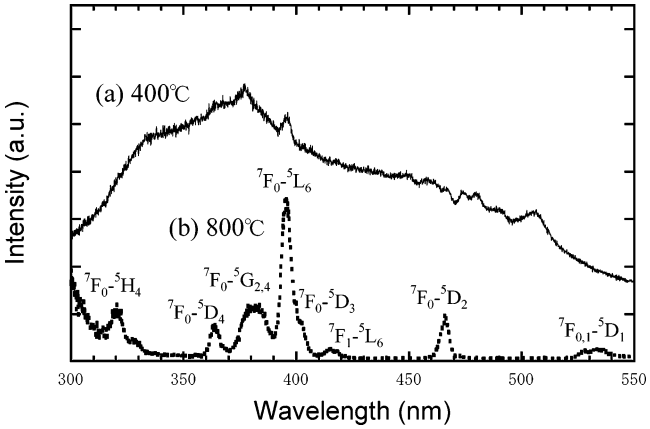


**Figure 8.** Excitation spectra monitored at 614 nm for AuEu−BS heated at (a) 400 and (b) 800 °C.

**TABLE 1: Enhancement Factor $f_E$ ($= R_{AuEu-B}/R_{Eu-BS}$) and Total Emission Intensities, $R_{AuEu-BS} = \Sigma_J I_J^{AuEu-BS}$ and $R_{Eu-BS} = \Sigma_J I_J^{Eu-BS}$, for AuEu−BS and Eu−BS, respectively, for Various Heating Temperatures[a]**

| temperature (°C) | $f_E$ | $R_{AuEu-BS}$ | $R_{Eu-BS}$ | $R_{C=O}$ |
|---|---|---|---|---|
| 200 | 2.56 | 2.56 | 1.0 | 1.0 |
| 400 | 6.08 | 58.9 | 9.68 | 2.35 |
| 600 | 0.76 | 0.77 | 1.01 | 0.33 |
| 800 | 2.45 | 6.91 | 2.82 | |

[a] These data are normalized by that of Eu−BS heated at 200 °C. The relative intensity $R_{C=O}$ of the broad band emission around 400 nm due to carbonyl groups, in comparison with that when heated at 200 °C, for various heat-treatment temperatures.

organics are completely removed and the PL intensities are increased again to the values about third times higher than at 200 °C. Additionally, $f_E$ is also increased to ~2.45. Because of the complete removal of PVP at the temperature, the factor $f_E$ of 2.45 shows a pure enhancement due to Au nanoparticles located in the vicinity of $Eu^{3+}$ ions.

## 4. Discussion

More recently, an energy transfer process from carbonyl groups to $Eu^{3+}$ ions in an organo-silicate gel is reported,[27] where the luminescence efficiency of $Eu^{3+}$ ions is greatly affected by forward and backward energy transfers between them. From our PL intensity data (Figure 6) and excitation spectra data (Figure 8) for various heating temperatures, a probable explanation of the enhancement of $Eu^{3+}$ fluorescence when sintered at low temperatures is given by the combination of enhanced local fields in the vicinity of Au nanoparticles and the energy transfer process from excited C═O groups to $Eu^{3+}$ ions in the ground state. The former causes the increasing population of the C═O groups in the excited state as well as the excited $Eu^{3+}$ ions. Figure 9 schematically illustrates the excitation and emission process of $Eu^{3+}$ ions. In the case (a) that no PVP and Au nanoparticles are introduced, $Eu^{3+}$ ions are excited through a charge transfer (CT) state by the wavelength of $\lambda = 337.1$ nm. After relaxation to $^5D_0$ level, the emissions due to $^5D_0$-$^7F_J$ transitions are obtained. If PVP is incorporated and the resultant gel is heated at temperatures around 400 °C (b), the coordinated C═O groups acts as energy donors to $Eu^{3+}$. The absorbed energy by singlet−singlet ($S_0 \rightarrow S_1$) transition of $\pi$ electrons of C═O groups is transferred to the $^5L_6$ levels of $Eu^{3+}$ ions through a triplet state of C═O. Interestingly, the $^5D_1$-$^7F_{1,2}$ emissions were obtained for the AuEu−BS sample heated at 400 °C, i.e., in case of the incorporation of the polymer-protected Au nanoparticles (see Figure 7). We found at the same time

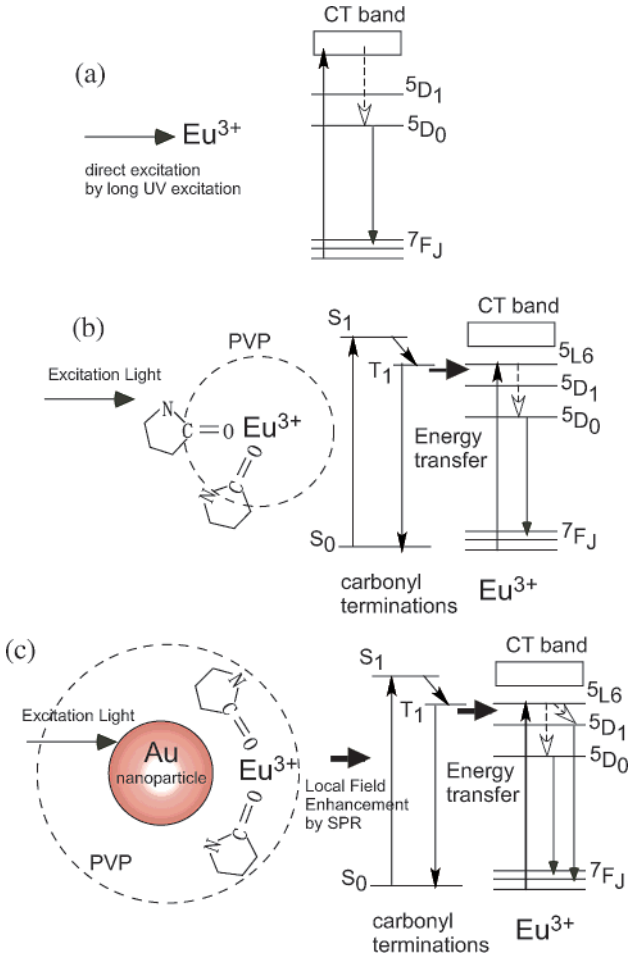


**Figure 9.** Schematical illustrations for enhanced $Eu^{3+}$ PL in the vicinity of PVP-protected Au nanoparticles. (a) Isolated $Eu^{3+}$ ions, (b) Eu−BS glass, and (c) AuEu−BS glass.

that $Eu^{3+}$ emissions were greatly enhanced in the presence of Au nanoparticles, and thus an influence of Au nanoparticles to $Eu^{3+}$ emissions is sufficient to be considered. Our data is therefore interpreted in such a way as the additional supplement of excitation energy for $Eu^{3+}$ ions was employed from C═O groups strongly excited in the local field enhanced by SPR of Au nanoparticles (see Figure 9c). This is also supported by the fact that the broad luminescence of C═O chromopheres was most intensified in the heat-treatment at 400 °C, as it can be seen as $R_{C=O}$ in Table 1. Indeed, the results in Table 1 also include an influence of hydroxyl (OH) vibration on the $Eu^{3+}$ luminescence efficiency. However, the observed enhancement of $Eu^{3+}$ luminescence cannot be explained only by this de-excitation.

It is important to point out that the incident light for excitation used in this work does not match with any resonance mode of surface plasmon, whose frequency is expressed by $\omega_L = \omega_p/(1 + (L + 1)/L\cdot\epsilon_M)^{1/2}$; the excitation energy is 3.68 eV, while an plasma oscillation of $L \rightarrow \infty$ occurs at the energy of 3.2 eV. Nevertheless, the strong excitation produce hot electrons through the $d \rightarrow sp$ interband transition, resulting in an increasing number of density of conduction electrons within a very short time of electron−phonon coupling time in pico-second order.[28] This simultaneously means a probable blue-shift of plasmon frequency $\omega_p$. Thus, we confidently propose that it is possible for the long UV light to derive a higher order of surface plasmon resonance for nanometer-sized Au particles, in the vicinity of which luminescent centers such as C═O chromophere or rare-earth ions can be strongly excited through the induced local field.

## 5. Conclusion

Nanometer-sized gold (Au) colloids in solution were incorporated into a borosilicate amorphous network of $10B_2O_3-90SiO_2$ together with $Eu^{3+}$ ions via a sol−gel route. To control the size and obtain good stability of Au nanoparticles a protective polymer of poly(vinylpyrrolidone) (PVP) was utilized throughout the synthesis. The sizes of the particles in a starting solution and gel-glasses were monitored by optical extinction spectra and analyzed by Mie-Drude theory. It was shown that $Eu^{3+}$ fluorescence of $^5D_0$-$^7F_J$ transitions in the vicinity of Au nanoparticles was enhanced by a local field enhancement due to higher orders of SPR excitations. The enhancement factor $f_E$ was ~2.5. Influences of carbon-related phosphors originating from the protective polymer for Au nanoparticles were also studied at various temperatures in heat-treatment for the fabricated gels of $10B_2O_3-90SiO_2$ doped with $Eu^{3+}$ ions. It was revealed that carbonyl groups around Au nanoparticles played a role of energy donor to $Eu^{3+}$ ions and further enhancement of $Eu^{3+}$ fluorescence, $f_E \sim 6$, was conclusively achieved. The enhancement will further be improved by modifying space-dispersion and size-distribution of Au nanoparticles in glasses.

**Acknowledgment.** A part of this work was carried out by the Nanotechnology Glass Project as part of Nanotechnology Materials Program supported by New Energy and Industrial Technology Development Organization (NEDO). T.H. gratefully acknowledges Nippon Sheet Glass Foundation for Materials Science and Engineering for financial support.

## References and Notes

(1) Born, M.; Wolf, E. *Principles of Optics*, 6th ed.; Pergamon: Oxford, 1980.
(2) Kittel, C. *Introduction of Solid State Physics*, 7th ed.; John Wiley & Sons: New York, 1996.
(3) Hache, F.; Ricard, D.; Flytzanis, C. *J. Opt. Soc. Am. B* **1986**, *3*, 1647.
(4) Ricard, D.; Roussignol, Ph.; Flytzanis, C. *Opt. Lett.* **1985**, *10*, 511.
(5) Uchida, K.; Kaneko, S.; Omi, S.; Hata, C.; Tanji, H.; Asahara, Y.; Ikushima, A. J.; Tokizaki, T.; Nakamura, A. *J. Opt. Soc. Am. B* **1994**, *11*, 1236.
(6) Das, P.; Metiu, H. *J. Phys. Chem.* **1985**, *89*, 4680.
(7) Chew, H. *J. Chem. Phys.* **1987**, *87*, 1355.
(8) (a) Malta, O. L.; Santos, M. A. Couto dos. *Chem. Phys. Lett.* **1990**, *174*, 13. (b) Malta, O. L.; Santa-Cruz, P. A.; De Sá, G. F.; Auzel, F. *J. Lumin.* **1985**, *33*, 261.
(9) Hayakawa, T.; Selvan, Tamil, S.; Nogami, M. *Appl. Phys. Lett.* **1999**, *74*, 1513.
(10) Hayakawa, T.; Selvan, Tamil, S.; Nogami, M. *J. Non-Cryst. Solids* **1999**, *259*, 16.
(11) Selvan, Tamil, S.; Hayakawa, T.; Nogami, M. *J. Phys. Chem. B* **1999**, *103*, 7064.
(12) Teranishi, T.; Kiyokawa, I.; Miyake, M. *Adv. Mater.* **1998**, *10*, 596.
(13) (a) Mayer, A.; Antonietti, M. *Colloid Polym. Sci.* **1998**, *276*, 769. (b) Toshima, N.; Harada, M.; Yamazaki, Y.; Asakura, K. *J. Phys. Chem.* **1992**, *96*, 9927. (c) Teranishi, T.; Hori, H.; Miyake, M. *J. Phys. Chem. B* **1997**, *101*, 5774.
(14) Mie, G. *Ann. Phys.* **1908**, *25*, 377.
(15) Doremus, R. H. *J. Chem. Phys.* **1964**, *40*, 2389.
(16) Doyle, W. T. *Phys. Rev.* **1958**, *111*, 1067.
(17) Epifani, M.; Carlino, E.; Blasi, C.; Giannini, C.; Tapfer, L.; Vasanelli, L. *Chem. Mater.* **2001**, *13*, 1533.
(18) Toki, M.; Chow, T. Y.; Ohnaka, T.; Samura, H.; Saegusa, T. *Polym. Bull.* **1992**, *29*, 653.
(19) Morikawa, A.; Iyoku, Y.; Kakimoto, M.; Imai, Y. *Polym. J.* **1992**, *24*, 687.
(20) Selvan, Tamil, S.; Hayakawa, T.; Nogami, M.; Möller, M. *J. Phys. Chem. B* **1999**, *103*, 7441.

(21) Kreibig, U.; Fragstien, C. v. *Z. Physik* **1969**, *224*, 307.
(22) Kreibig, U.; Vollmer, M. *Optical Properties of Metal Clusters*; Springer: Berlin, 1995.
(23) Cooper, B. R.; Ehrenreich, H.; Philipp, H. R. *Phys. Rev.* **1965**, *2*, A494.
(24) (a) Hovel, J.; Fritz, S.; Hilger, A.; Kreibig, U.; Vollmer, M. *Phys. Rev.* **1993**, *48*, 18278. (b) Alemany, P.; Boorse, R. S.; Burlitchmad, J. M.; Hoffman, R. *J. Phys. Chem.* **1993**, *97*, 8464. (c) Hayakawa, T.; Ono, Y.; Nogami, M. *Proc. SPIE* **2000**, *3943*, 102.
(25) Canham, L. T.; Loni, A.; Calcott, P. D. J.; Simons, A. J.; Reeves, C.; Houlton, M. R.; Newey, J. P.; Nash, K. J.; Cox, T. I. *Thin Solid Films* **1996**, *276*, 112.
(26) Levy, D.; Reisfeld, R.; Avnir, D. *Chem. Phys. Lett.* **1984**, *109*, 593.
(27) Molina, C.; Dahmouche, K.; Messaddeq, Y.; Ribeiro, S. J. L.; Silva, M. A. P.; de Zea Bermudez, V.; Carlos, L. D. *J. Lumin.* **2003**, *104*, 83.
(28) (a) Hamanaka, Y.; Hayashi, N.; Nakamura, A.; Omi, S. *J. Lumin.* **1998**, *76&77*, 221. (b) Inouye, H.; Tanaka, K.; Takahashi, I.; Hirao, K. *Phys. Rev. B* **1998**, *57*, 1134.